On the design of Latent Thermal Energy Storage Solutions for Buildings: From Materials to Applications

Dario GUARDA[1], Giacomo FAVERO[1], Gianluca SLAVIERO[1], Giulia RIGHETTI[1], Claudio ZILIO[1], Luca DORETTI[2], Simone MANCIN[1,*]

[1]University of Padova, Department of Management and Engineering, Vicenza, Italy
[1]University of Padova, Department of Civil, Environmental and Architectural Engineering, Padova, Italy

dario.guarda@unipd.it, giacomo.favero.1@phd.unipd.it, gianluca.slaviero@phd.unipd.it, giulia.righetti@unipd.it, claudio.zilio@unipd.it, luca.doretti@unipd.it, simone.mancin@unipd.it

* Corresponding Author

ABSTRACT

Future smart and efficient energy management systems for space cooling and heating in building applications require novel solutions to store heat to decouple the energy demand and the availability of renewable energy sources. Latent thermal energy storages represent one of the most promising solutions; however, their cost-effective implementation in terms of energy and cost savings and payback time needs to be verified case by case. Moreover, the design of these components is not simple because the heat transfer process involves the solid/liquid phase change that deeply affects the storage heat transfer capability. This work presents an outlook on the importance of the scaling up of the research to deploy efficient and smart solutions for novel latent thermal energy storage systems. The paper explores the work done by the Thermal Energy Innovation research group from a few grams to hundreds of kilograms of organic phase change materials showing original and novel experimental and numerical results.

1. INTRODUCTION

Decarbonization of heating and cooling is imperative for climate change mitigation (IRENA 2023). According to the IEA report (2020), approximately 37 Gton of CO_2 were estimated to have been released into the atmosphere during 2019. A similar value was obtained for 2020. It is absolutely essential to reduce this figure, calling researchers to focus on finding and developing innovative solutions. A huge amount of energy is used for space heating and cooling, and, in the last decades, energy management and indoor thermal comfort have become challenging issues. Gagliano *et al.* (2012) reported that in European Countries the total cooled floor area is expected to grow up to 2 billion m^2 in 2020 (it was 1000 million m^2 in 2012). Therefore, more than 100 TWh $year^{-1}$ will be required for building cooling only.
For this purpose, the utilization of heat pumps driven by electricity from renewable energy sources can reduce the carbon foot print of heating and cooling (Poppi *et al.* 2018). However, the mismatch between the availability of renewable energy sources, such as photovoltaic electricity, and heating and cooling demand limits the effective utilization of renewable energy.
In a recent critical review work, Cabeza and Chafer (2020) reported the passive and active strategies needed to achieve zero energy buildings. Among other solutions, the presence of energy storages has been recommended. Thermal Energy Storage (TES) can be considered an enabling technology to promote a great and more efficient adoption of renewable sources which are one of the solutions to reduce the GHG emissions. TES technologies can be commonly classified into three types: sensible, latent, and thermochemical (Sharma *et al.*, 2009). Compared to other types of TES, Latent Thermal Energy Storages (LTESs) equipped with Phase Change Materials (PCMs) exhibit many advantages. In fact, as described by Colla *et al.* (2017), due to the latent heat of fusion, the LTES energy storage density capability is remarkably higher compared to sensible-only TES systems. Taking into account the same temperature range, when using LTES, from 5 to 8 times the energy of a sensible thermal energy storage system can be stored in the same volume; in addition, the phase change process can be considered almost isothermal (Lazzarin *et al.* 2017). These characteristics permit to maximize both the storage capabilities and the heat transfer process. It is

also important to note that the use of PCMs allows for the decoupling between energy demand and availability; this point is of fundamental interest for the effective integration of renewable sources that are intermittent by definition. These features allow LTES and PCMs to be suggested in many applications, such as thermal management (Zhou *et al.*, 2012), HVAC systems (Rastogi *et al.*, 2015), electrical energy generation (Jing *et al.* 2010), thermal energy recovery (Shon *et al.,* 2014 and Xu *et al.* 2017), thermal management of electronic devices and batteries of electric vehicle batteries (Ren *et al.* 2020 and Verma *et al.* 2019) or refrigerated transport in the cold chain (Calati *et al.* 2022). One of the most interesting applications of this technology is in the air conditioning (i.e. space cooling) field, in which the possibility of a direct integration of the LTES with an air/water or water/water heat pump powered by photovoltaics (PVs) can lead to huge energy savings by matching the energy source availability with the cooling demand, which are commonly mismatched (Gagliano *et al.* 2012 and Cabeza *et al.* 2020). This is particularly true, especially in hot and humid climates.

In the last decade, many different passive and active systems, have been proposed for space heating and cooling, as well as for domestic hot water. In fact, as clearly appears from the open literature, many experimental studies on LTES have already been published to analyze the effects of different enhancement methods (e.g., metal foams, finned surfaces) on the heat transfer performance of the PCM, but almost all of them involve small amount of PCM (Lazzarin *et al.* 2018, Righetti *et al.* 2020a, 2020b, 2021, Zhang *et al.* 2022, Mancin *et al.* 2015].

Figure 1 shows a few examples of small-scale studies carried out at the Thermal Energy Innovation (TEI) research group at the University of Padova. Figure 1(a) shows the activities on 3D periodic structures containing form 50-60 g of PCM, while Figure 1(b) presents the use of X-ray computed tomography to study the solid-liquid phase change of possible salt hydrate candidates (30 g) for space heating. Finally, Figure 1(c) reports two visualizations of the phase change process occurring inside a tube in tube heat exchanger with topologically optimized fins to enhance the solid-liquid phase change of 500 g of PCM. It is hard thinking that from these experimental studies, it would be possible to extrapolate information that can be applied to large-scale LTES systems.

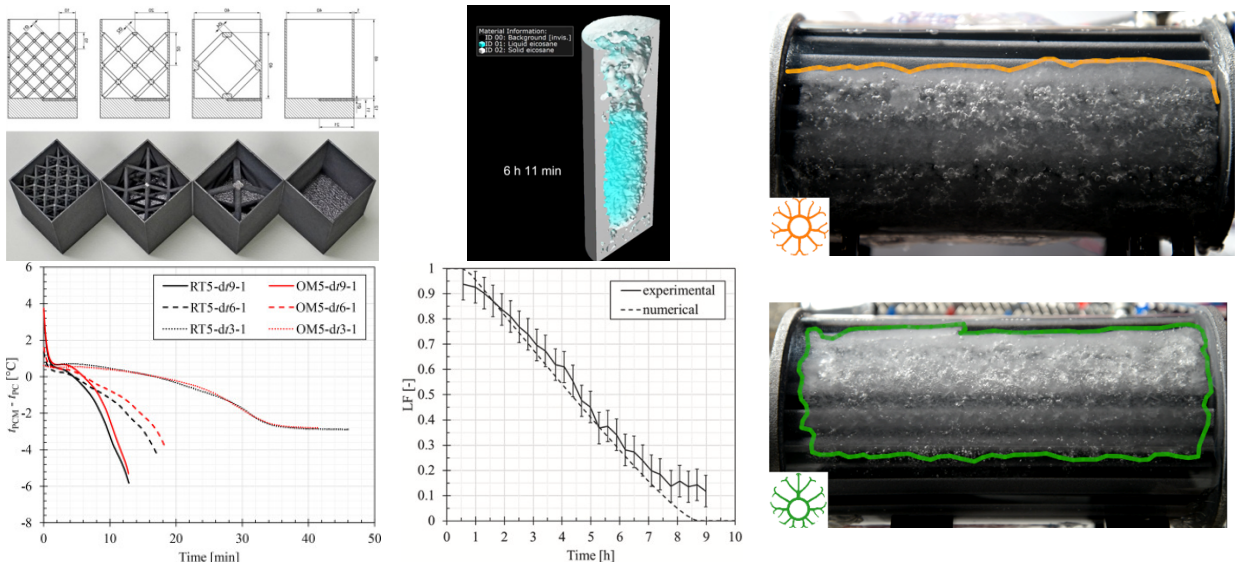

(a) (b) (c)

Figure 1: Recent example of research activities at TEI research group: (a) 3D periodic structures for solid-liquid phase change enhancement (Guarda *et al.*, 2023a); (b) X-ray computed tomography of salt hydrates solid-liquid phase change (Guarda *et al.,* 2023b); (c) Topology optimization of finned surfaces for solid-liquid phase change enhancement (Favero *et al.,* 2024).

In general, there is a lack of understanding if the data collected in small-scale prototypes can be used to anticipate the performance of the systems at larger scale; moreover, it is also not clear so far if the models developed and validated on the basis of these results are representative to simulate the behavior of LTES at system or building level.

This work aims at presenting a novel 18 kWh LTES especially designed for space cooling, which uses the roll-bond technology to efficiently store and release the energy exploiting the solid/liquid phase change process of a commercially available biobased PCM, CRODATHERM9.5.

The roll-bond heat exchanger is a simple, almost inexpensive cold (hot) plate that can be easily used in any type of LTES due to its versatility. It can be produced in different sizes and allows for a direct scalability of both capacity and heat transfer capabilities of the LTESs.

2. MATERIALS AND METHODS

2.1 The PCM

This PCM is a water insoluble organic PCM derived from plant-based feedstocks and has the form of a crystalline wax or oily liquid (depending on temperature). This material is completely biocompatible and biodegradable. Its main thermophysical properties are listed in Table 1. The phase-change temperature peak is at around 9 °C and the latent heat is 220 kJ/kg. Moreover, Longo *et al.* (2022) measured the thermal conductivity and the dynamic viscosity of several organic PCM, including the CRODATHERM9.5.

Table 1. PCM thermophysical properties (values reported by CRODA).

Property	Value	Unit
Density at 2°C	963	kg m^{-3}
Density at 20°C	858	kg m^{-3}
Flash point	195	°C
Specific heat capacity (solid)	2.2	kJ $kg^{-1}K^{-1}$
Specific heat capacity (liquid)	2.1	kJ $kg^{-1}K^{-1}$
Thermal conductivity (solid)	0.24	W $m^{-1}K^{-1}$
Thermal conductivity (liquid)*	0.158	W $m^{-1}K^{-1}$
Peak melting temperature	9	°C
Total stored heat from 1 to 16 °C	220	kJ kg^{-1}
Peak crystallization temperature	9	°C
Total stored heat from 16 to 1 °C	216	kJ kg^{-1}
*Measured/confirmed by Longo *et al.* (2022)		

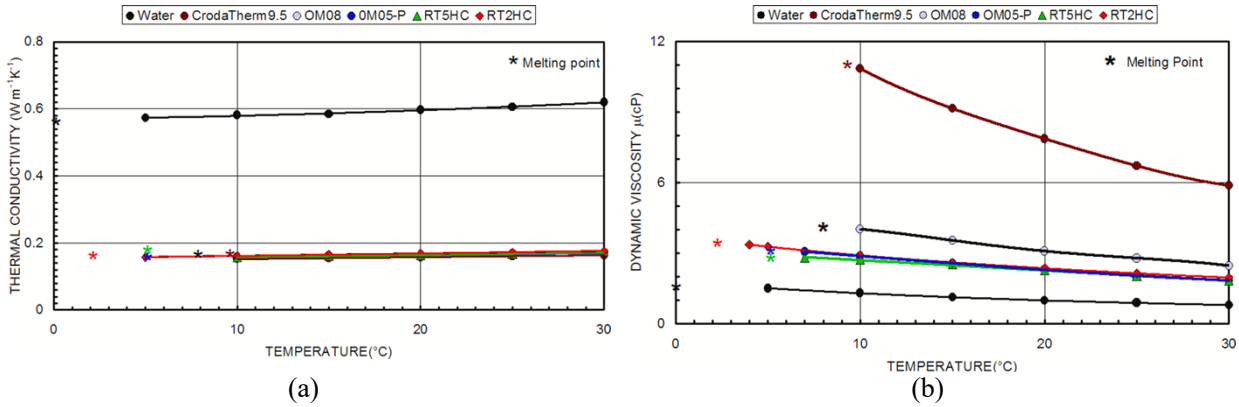

(a) (b)

Figure 2: Thermophysical properties of organic PCM, including also CRODATHERM9.5 measured by Longo *et al.* (2022). (a) Thermal conductivity and (b) Dynamic viscosity as a function of the temperature.

The thermal conductivity of the CRODATHERM9.5 is close to those of the other organic PCMs, while the dynamic viscosity is from 7.4 to 8.3 times higher than those of water. Dynamic viscosity is of great importance because it affects the natural motions inside the liquid PCM during phase change. In general, a high viscosity inhibits natural convection and thus it limits the heat transfer during phase change. Thus, in the present case study, it can be expected that the natural convection could potentially be inhibited.

2.2 Experimental setup

A specific setup was built to perform the experimental characterization of the LTES under study. Figure 3 shows a schematic of the experimental apparatus. It consists of an off-the-shelf storage tank with internal dimensions of 1400 mm × 710 mm × 650 mm. The wall contains 50 mm of insulation to limit heat losses to the surroundings, covered with an aluminum sheet. The tank is filled with 300±0.5 kg of CRODATHERM9.5, supplied by CRODA.

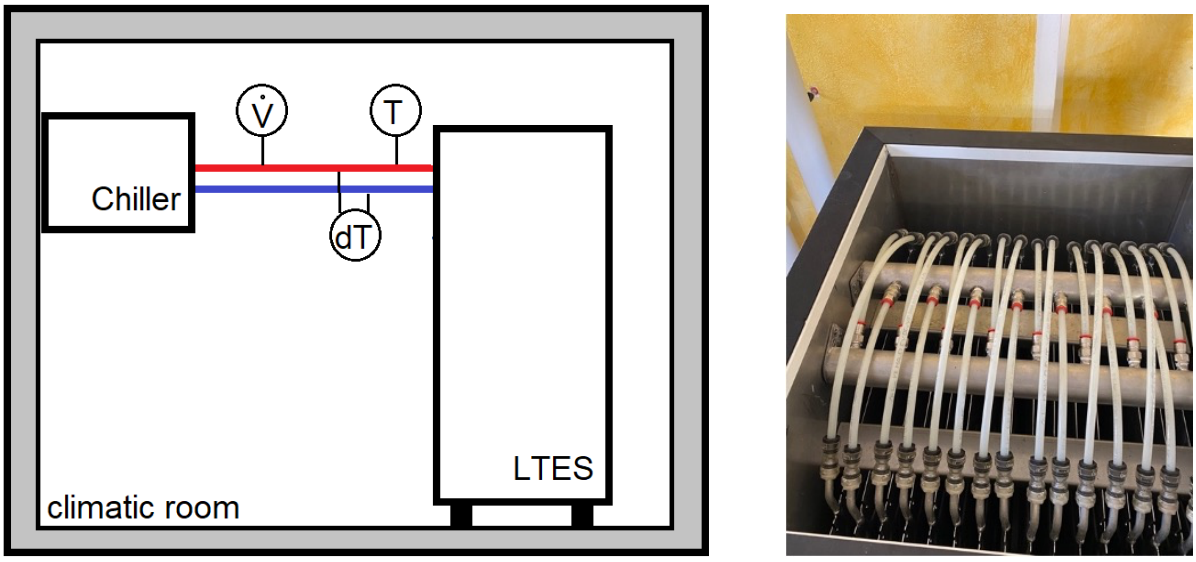

(a) (b)

Figure 3: (a) Experimental set up scheme. (b) A picture of the roll-bond based TES depicting the heat exchangers' arrangement.

As it can be seen in Figure 3(b), inside the tank there are 16 roll-bond heat exchangers made of aluminum having dimensions 1170 mm × 570 mm × 1.5 mm. The heat exchanger pitch is 31 mm and it is filled with PCM. The roll-bonds allow the passage of hot and cold water and, because of the presence of a continuous aluminum plate, they promote heat transfer within the PCM that has a relatively low thermal conductivity, similar to the large majority of PCMs. Roll-bond heat exchangers are fed in pairs in parallel by two manifolds located on the top of the tank.

Roll-bond technology is an efficient and performant solution which has been implemented for decades in refrigeration industry. It produces one of the thinnest flat (only 1.5 mm in thickness) heat exchangers, consisting of two sheets of aluminum bonded at very high pression while leaving an appropriate designed inked circuit between the two layers. The bonded plate is then inflated by compressed air to create a channel between the two sheets of aluminum. The heat transfer fluid (in this case water) circulates into this circuit and it activates the aluminum flat panel, which assumes an average temperature similar to that of the fluid. This type of heat exchanger represents a possible cheap and efficient solution for the LTES application. Aluminum panels are light and can be easily positioned as batteries in the container internal volume. In the open literature, only a few papers proposed the use of roll-bond heat exchangers coupled with PCM. Roll-bond technology is commonly applied to refrigeration systems such as evaporators. However, a few different PCM applications have also been proposed. For example, roll-bond technology was applied to hybrid PCM+PV/T systems, because PCMs have

been shown to be a very effective cooling medium to limit the temperature of the PV module and the roll-bond geometry is suitable for combined with PV/T panels. The water flowing inside the inlet manifold is supplied by an external thermostatic bath that can independently regulate the flow rate and the inlet temperature. The volumetric flow rate is measured by an Endress + Houser Promag H electromagnetic flow meter with an accuracy of ±0.5% of the full scale (full scale 40 l min^{-1}). The inlet water temperature is measured with a calibrated T-type thermocouple (copper-constantan) with uncertainty (coverage factor k=2) equal to ±0.1 K since it is connected to a Kaye K170 Ice Point Reference with stability of ±0.005 °C and accuracy of ±0.005 °C. A thermopile with uncertainty (coverage factor k=2) of ±0.05 K measures the temperature difference between the water inlet and the outlet.
Additionally, 39 calibrated T-type thermocouples (uncertainty ±0.1 K) were immersed inside the PCM. They were located using 11 stainless steel rods at 5 different heights. In this way, it was possible to analyze the temperature field during the experimental tests.
All data were acquired using a Keysight 34970A acquisition system with a sampling rate of 1 Hz (uncertainty on the reading time span of the reading ±0.001 s). The data are then processed using LabView software.
The tank was placed inside a climatic room whose temperature was maintained during all tests at 9.0±0.2 °C to avoid heat losses from the tank to the environment.
Repeatability tests were conducted for some operating conditions; each selected operating condition was repeated 4 times. Percentage differences below ±2% were observed for the total charging and discharging times (total charging + discharging time from 1004 to 1023 min). For the definition of the charging and discharging times, see the section "3.1 charging and discharging time definition" section. The thermal balance between charging and discharging phases was always checked, and, for example, considering a complete cycle, the amounts of energy stored in the charging and discharging were 18.5 and 18.3 kW (maximum difference of about 2%), respectively.
The energy stored in the LTES (E) is calculated starting from the power (P) exchanged by the water, evaluated according to Eq.1. The instant power is then integrated over the cycle to obtain the energy exchanged by the water in the interval between two readings (Eq. 2).

$$P = \dot{m}\, c_p\, (t_{in} - t_{out}) \tag{1}$$

$$E = \int_{\tau_0}^{\tau_f} P \cdot \mathrm{d}t \tag{2}$$

Since the climatic chamber is set at 9±0.2 °C and the temperature of the LTES during phase change is about 9 °C, it can be assumed that heat losses can be neglected.
In fact, they were estimated to be less than 2%. This value was obtained by comparing the energy given by the water, measured according to equations 1 and 2 (that was between 18.5 and 18.3 kW depending on the test) and the energy stored by the LTES. This value was evaluated taking the PCM enthalpy variation of 210 kJ/kg for a temperature change from 14 °C to 7 °C (as declared by the manufacturer), a PCM specific heat equal to 2.1 kJ/kg K (see Table 1) and an aluminum specific heat equal to 0.880 kJ/kg K. From the calculations, the energy stored by the system is given by the sum of three contributions: PCM latent heat of 17.5 kWh, PCM sensible heat of 1.1 kWh, and aluminum sensible heat of about 0.1 kWh. The result is about 18.7 kWh.
Furthermore, according to the Kline and McClintock (1953) method, the uncertainty on total energy stored was evaluated to be maximum ±3.1% and on average ±1.5%.

3. RESULTS AND DISCUSSION

In general, a typical test consists of a charging phase and a discharging phase. At the beginning of the (cold) energy charging phase, the PCM is liquid. During the charging phase, the LTES stores cold energy from the cold inlet water that flows inside the roll-bond heat exchangers until the solidification process is completed. In the (cold) discharging

phase, the solid PCM releases the cold energy that had been stored to the warmer water that flows inside the roll-bonds. At the end of the discharging phase, the PCM is fully liquefied again.
At first, charging and discharging tests were run under the reference rating conditions suggested by the supplier. The cold energy absorbed and released during the phase change processes and the temperature field recorded by the 39 thermocouples were collected and analyzed.
Then, since these LTESs should meet a demand for a non-constant energy supply over time, additional tests were carried out to compare the behavior during continuous and batch discharging phases.
The (cold) energy charging test started when the LTES had an average temperature of 14°C. Cold water flowed through the roll-bond heat exchangers at an inlet temperature of 2 °C and a flow rate of 17 l min^{-1}, which are the reference rating conditions. The test ended when all the thermocouples inside the PCM recorded a temperature of 7 °C, that is, 2 K lower than the PCM phase change temperature. The (cold) energy discharging test began immediately thereafter; the average temperature of the PCM under these conditions was 6 °C. An equal water flow rate (17 l min^{-1}) at a temperature of 16 °C flowed inside the heat exchangers until the PCM reached an average temperature of 14 °C, 2 K lower than the inlet water temperature. During this test, the climatic chamber was kept at 9 °C to limit the heat loss to the surroundings.
Figure 4 reports the complete charging and discharging cycle collected at constant water flow rate of 17 l min^{-1} and inlet water temperature equal to 2°C and 16°C during the charging and discharging phases, respectively. Multiple charging and discharging cycles were run and a high repeatability were found; thus, for the sake of clarity, only one test is here reported here.
Considering the curve plotted in Figure 4, during the charging phase 17.68 kWh of cold energy were stored, while during the discharging phase 17.39 kWh of cold energy were released. This means that the energy balance between charging and discharging is about 300 Wh, less than 2% of the total energy stored.

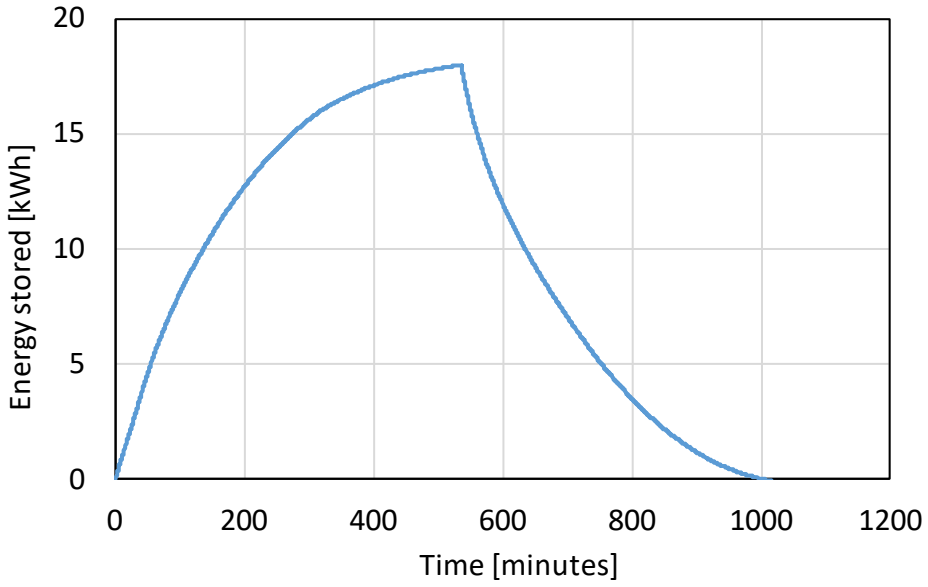

Figure 4: Cold energy stored and released during the entire cycle as a function of the time at a constant water flow rate of 17 l min^{-1}. The inlet water temperature was equal to 2 °C and 16 °C during the charging and discharging phases, respectively.

Figure 5(a) shows the histogram of the hourly cold energy stored inside the LTES during the charging phase, while Figure 5(b) shows the same information during the discharging phase. From the results, one can immediately notice that during the first hour the LTES is able to store (and release) more than 30% of the cold energy; then, the heat transfer performance decreases but in the first 4 hours the LTES stores (and release) more than 75% of the energy. This means that, in a real case application, this LTES can be very efficient during the first working hours, but then, the performance will worsen with time. However, the roll-bond technology seems to enhance heat transfer during the phase change and to mitigate, at least during the first 4 hours, the low thermal conductivity and the high dynamic viscosity of CRODATHERM9.5 as compared to an ideal case without any extended surfaces.

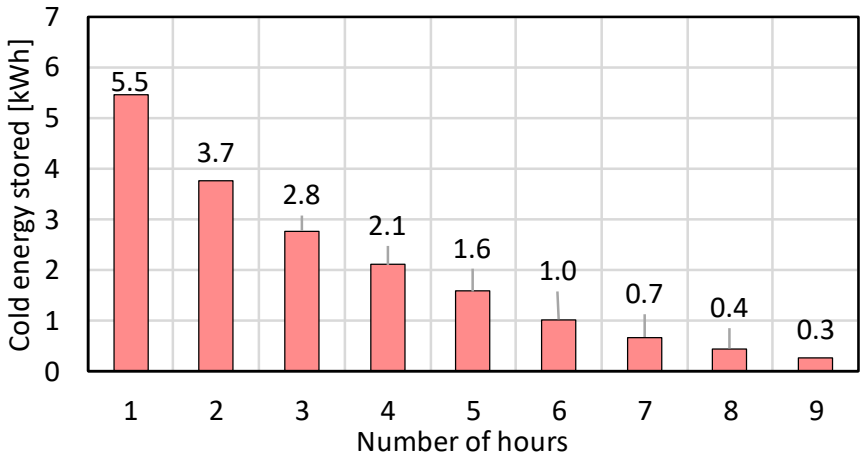

(a)

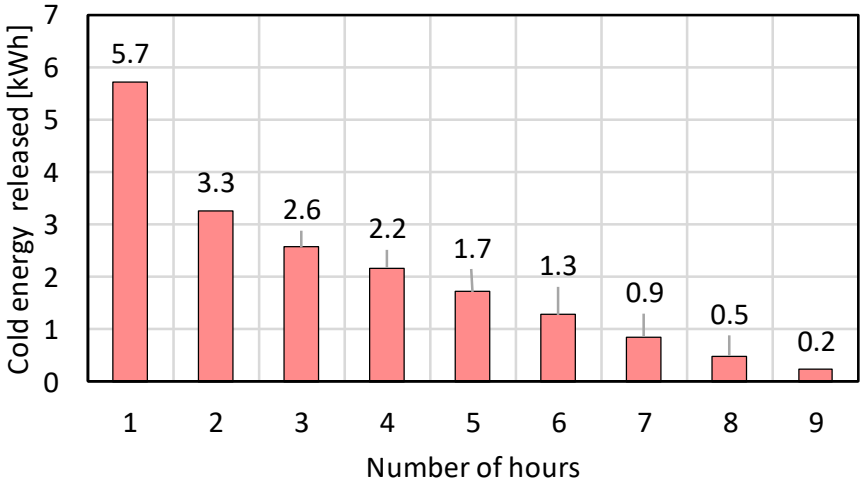

(b)

Figure 5: Energy stored and released hourly during charging (a) and discharge (b) at a constant water flow rate of 17 l min^{-1}. The inlet water temperature was equal to 2 °C and 16 °C during the charging and discharging phases, respectively.

Figure 6 shows the temperature profiles inside the PCM during charging (Figure 6(a)) and discharging (Figure 6(b)). It should be pointed out that temperatures measured on plane 1 were not reported on the graphs because they were affected by the presence of air due to the PCM volume shrinking during the solidification. Moreover, it was decided to plot only the average temperatures evaluated on each plan.

Due to the symmetry of the tank, differences lower than ±1 K were found between thermocouples located in the same plane. In contrast, this system presents strong vertical temperature stratification during the cooling and heating phases. The lowest plane (5) is located 3 cm from the bottom of the tank, even lower than the last roll-bond channel, where the water flows. It is the first to cool down, most likely due to the convective movements generated inside the tank. In fact, the density increases with decreasing temperature. Then, all the other planes reach the phase-change temperature in a sequential order. After about 40 min, the whole PCM is storing only latent heat. It is possible to measure a subcooling of about 1.6 °C, more evident in the lower planes, before starting the solidification process. Liu *et al.* (2012) also observed a subcooling effect in a large storage of PCM with a melting temperature of -26.7 °C.

The LTES is undoubtedly useful to decouple energy demand from the availability of the energy sources. Furthermore, it is not necessarily the case that the cold energy demand is constant over time.

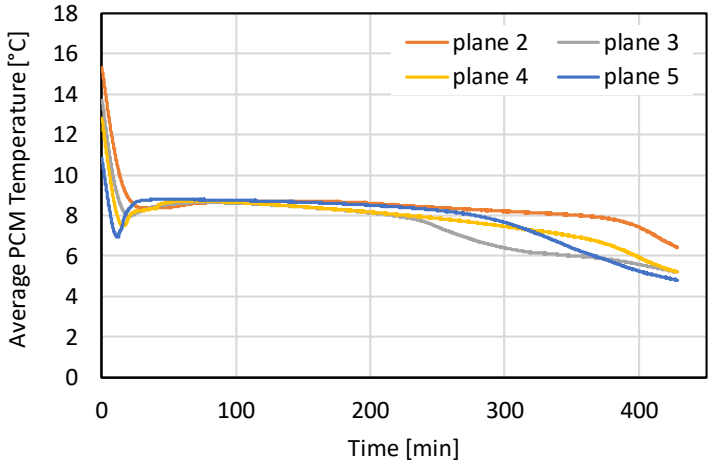

(a)

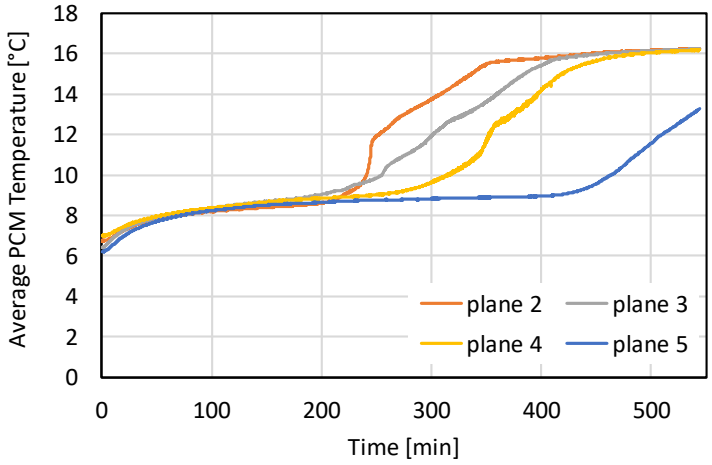

(b)

Figure 6: Energy stored and released hourly during charging (a) and discharge (b) at a constant water flow rate of 17 l min^{-1}. The inlet water temperature was equal to 2 °C and 16 °C during the charging and discharging phases, respectively.

6. CONCLUSIONS

This work presents an experimental assessment of a novel 18 kWh LTES based on roll-bond technology, which uses a biobased PCM CRODATHERM9.5 specifically developed for air conditioning applications. The charging and discharging phases are investigated by varying the water flow rate and the inlet water temperature and by monitoring the phase change process using 39 thermocouples inserted inside the PCM storage and the cold energy stored in the LTES. From the collected results, it can be stated that: at 17 l min^{-1} and setting the inlet water temperature at 2°C, the total charging time was 512 min, while the total discharging time was 618 min and it was also observed that 75% of the energy is stored/released during the first 4 hours. Therefore, it is recommended to maximize the storage capabilities of the LTES in this time frame.

The temperature of the PCM was monitored inside the LTES using 39 thermocouples placed on 11 rods at 5 different heights. The temperature was found to be homogeneous in each plane, while a vertical temperature gradient was observed, mainly due to convective motions inside the liquid.

To conclude, these results showed that this technological solution allowed to store cold energy and then release it when needed; in this way, it is possible to efficiently decouple the availability of renewable energy sources from the cooling demand.
The collected experimental measurements can be considered one of the first databases that collects temperature distributions during the phase change process, and energy-stored profiles of a real-scale LTES for air conditioning, allowing for the development and validation of both local numerical simulations of the LTES when integrated in a complex heating/cooling energy system equipped with heat pump and solar PV/T array for household applications. Future efforts will surely be needed to develop and verify active control strategies to optimize the performance of the LTES-Heat Pump integrated system; otherwise, the beneficial opportunities offered by the energy storage technologies can vanish.

NOMENCLATURE

c_p	specific heat capacity	(J/kg.K)
E	energy	(J)
$\dot{m}$	mass flow rate	(kg/s)
P	power	(W)
t	temperature	(°C)

Subscript

0	initial
F	final
in	inlet
out	outlet

Abbreviations

LTES	latent thermal energy storage
PCM	phase change material
PV	photovoltaic
PV/T	photovoltaic/thermal panel
TES	thermal energy storage

REFERENCES

Cabeza, L.F. & Chàfer, M. (2020). Technological options and strategies towards zero energy buildings contributing to climate change mitigation: A systematic review, *Energy Build*. 219, 110009

Calati, M., Zilio, C., Righetti, G., Longo, G.A., Hooman, K. & Mancin, S. (2022). Latent thermal energy storage for refrigerated trucks, *International Journal of Refrigeration.* 136, 124–133.

Colla, L., Ercole, D., Fedele, L., Mancin, S., Manca, O. & Bobbo, S. (2017). Nano-phase change materials for electronics cooling applications, *J Heat Transfer*. 139, 1–9.

International Energy Agency IEA, (2020). www.iea.org.

IRENA. 2023. *Innovation Landscape for Smart Electrification: Decarbonising End-Use Sectors*. Abu Dhabi: International Renewable Energy Agency.

Favero, G., Slaviero G., Zhang, S., Righetti, G., Pu, L. & Mancin S. (2024). Experimental and numerical study of solid/liquid phase change of paraffin in 3d printed axially finned tubes obtained through topological optimization, Proc. of the Eurotherm conference, Slovenia.

Gagliano, A., Patania, F., Nocera, F., Ferlito, A. & Galesi, A. (2012). Thermal performance of ventilated roofs during summer period, *Energy Build*. 49, 611–618.

Guarda, D., Righetti, G., Longo, G.A., Zilio, C. & Mancin, S. (2023a). Experimental assessment of low temperature phase change materials (PCM) for refrigerating and air conditioning applications, *International Journal of Refrigeration,* 154, 33-42.

Guarda, D., Martinez-Garcia, J., Fenk, B., Schiffmann, D., Gwerder, D., Stamatiou, A., Worlitschek, J., Mancin, S. & Schuetz, P. (2023b). New liquid fraction measurement methodology for phase change material analysis based on X-ray computed tomography, *International Journal of Thermal Sciences*, 194, 108585.

Jing, L., Gang, P., Jie, J. (2010). Optimization of low temperature solar thermal electric generation with Organic Rankine Cycle in different areas, *Appl Energy.* 87, 3355–3365

Kline, S. & McClintock, F. (1953). Describing uncertainties in single sample experiments, *Mechanical Engineering*. 75, 3–8.

Lazzarin, R.M., Mancin, S. Noro, M. & Righetti, G. (2018). Hybrid PCM-aluminium foams' thermal storages: An experimental study, *International Journal of Low-Carbon Technologies*. 13, 286–291.

Liu, M., Saman, W. & Bruno, F. (2012), Development of a novel refrigeration system for refrigerated trucks incorporating phase change material, *Appl Energy*. 92, 336–342.

Longo, G.A., Mancin, S., Righetti, G. & Zilio, C. (2022). Experimental measurement of thermophysical properties of some commercial phase change materials (PCM) for air conditioning applications, *International Journal of Refrigeration*, 144, 202-210

Mancin, S., Diani, A., Doretti, L., Hooman, K. & Rossetto, L. (2015). Experimental analysis of phase change phenomenon of paraffin waxes embedded in copper foams, *International Journal of Thermal Sciences.* 90, 79–89.

Poppi, S., Sommerfeldt, N., Bales, C., Madani, H. & Lundqvist, P. 2018. "Techno-Economic Review of Solar Heat Pump Systems for Residential Heating Applications." *Renewable and Sustainable Energy Reviews* 81, 22–32.

Rastogi, M., Chauhan, A., Vaish, R. & Kishan, A. (2015) Selection and performance assessment of Phase Change Materials for heating, ventilation and air-conditioning applications, *Energy Convers Manag*. 89, 260–269.

Ren, Q., Guo, P. & Zhu, J. (2020). Thermal management of electronic devices using pin-fin based cascade microencapsulated PCM/expanded graphite composite, *Int J Heat Mass Transf.* 149, 119199.

Righetti, G., Savio, G., Meneghello, R., Doretti, L. & Mancin, S. (2020a). Experimental study of phase change material (PCM) embedded in 3D periodic structures realized via additive manufacturing, *International Journal of Thermal Sciences.* 153.

Righetti, G., Zilio, C., Doretti, L., Longo, G.A. & Mancin, S. (2020b). Experimental investigation of phase change of medium/high temperature paraffin wax embedded in 3D periodic structure, *International Journal of Thermofluids*. 5–6, 100035

Righetti, G., Zilio, C., Doretti, L., Longo, G.A. & Mancin, S. (2021). On the design of Phase Change Materials based thermal management systems for electronics cooling, *Appl Therm Eng.* 196, 117276.

Sharma, A., Tyagi, V. V., Chen, C.R. & Buddhi, D. (2009). Review on thermal energy storage with phase change materials and applications, *Renewable and Sustainable Energy Reviews*. 13, 318–345.

Shon, J., Kim, H. & Lee, K. 2014. Improved heat storage rate for an automobile coolant waste heat recovery system using phase-change material in a fin–tube heat exchanger, *Appl Energy*. 113, 680–689.

Xu, H., Romagnoli, A., Sze, J.Y. & Py, X. 2017. Application of material assessment methodology in latent heat thermal energy storage for waste heat recovery, *Appl Energy*. 187, 281–290.

Verma, A., Shashidhara & S., Rakshit, D. 2019. A comparative study on battery thermal management using phase change material (PCM), *Thermal Science and Engineering Progress*. 11, 74–83.

Zhang, S., L. Pu, L, S. Mancin, S., Dai, M. & Xu, L., 2022, Role of partial and gradient filling strategies of copper foam on latent thermal energy storage: An experimental study, *Energy*, 255, 124517.

Zhou, D., Zhao, C.Y. & Tian, Y., 2012. Review on thermal energy storage with phase change materials (PCMs) in building applications, *Appl Energy*, 92, 593–605.